Biol Trace Elem Res (2016) 173:390–398
DOI 10.1007/s12011-016-0668-5

Bis(maltolato)oxovanadium(IV) (BMOV) Attenuates Apoptosis in High Glucose-Treated Cardiac Cells and Diabetic Rat Hearts by Regulating the Unfolded Protein Responses (UPRs)

Xiao-Qiang Cong[1] · **Mei-Hua Piao**[2] · **Ying Li**[3] · **Lin Xie**[4] · **Ya Liu**[4]

Received: 5 January 2016 / Accepted: 6 March 2016 / Published online: 16 March 2016

Abstract Endoplasmic reticulum stress (ERS)-induced unfolded protein response (UPR) and the subsequent cell deaths are essential steps in the pathogenesis of diabetic cardiomyopathy (DCM), a main cause of diabetics' morbidity and mortalities. The bis(maltolato)oxovanadium(IV) (BMOV), a potent oral vanadium complex with anti-diabetic properties and insulin-mimicking effects, was shown to improve cardiac dysfunctions in diabetic models. Here, we examined the effects of BMOV on UPR pathway protein expression and apoptotic cell deaths in both high glucose-treated cardiac H9C2 cells and in the hearts of diabetic rats. We show that in both the high glucose-treated cardiac cells and in the hearts of streptozotocin (STZ) diabetic rats, there was an overall activation of the UPR signaling, including both apoptotic (e.g., the cascades of PERK/EIf2α/ATF4/CHOP and of IRE1/caspase 12/caspase 3) and pro-survival (GRP78 and XBP1) signaling. A high amount of apoptotic cell deaths was also detected in both diabetic conditions. The administration of BMOV suppressed both the apoptotic and pro-survival UPR signaling and significantly attenuated apoptotic cell deaths in both conditions. The overall suppression of UPR signaling by BMOV suggests that the drug protects diabetic cardiomyopathy by counteracting reactive oxygen species (ROS) and endoplasmic reticulum (ER) stress. Our findings lend support to promote the use of BMOV in the treatment of diabetic heart diseases.

Keywords Diabetic cardiomyopathy · Unfolded protein response · Apoptosis · Bis(maltolato)oxovanadium(IV) (BMOV) · H9C2 cells · Diabetic rats

Introduction

Cardiomyopathy independent of major vascular diseases is becoming one of the main complications of diabetes, resulting in a high percentage of morbidity and mortality [1]. According to a recent report, 56 % of the diabetes patients have diabetic cardiomyopathy (DCM), and cardiac dysfunctions have become the leading cause of death in the diabetic population [2]. Apoptotic cell death has been reported to play a critical role in the development of diabetic cardiomyopathy [1, 3–5]. Increasing evidence suggest that the endoplasmic reticulum (ER) stress (ERS)-induced unfolded protein responses (UPRs) are essential steps in the pathogenesis of diabetic cardiomyopathy [6, 7]. For example, Li et al. [8] demonstrated that ER stress was involved in the cardiac apoptosis of a streptozotocin (STZ)-induced type 1 diabetic rat model. A number of studies observed the upregulation of UPR pathway proteins in the hearts of diabetic models, such as PERK, ATF6, p-EIf2, cleaved ATF6 and GRP78, etc. [4, 8–12]. Younce et al. reported that high glucose caused cardiomyopathy via reactive oxygen species (ROS) production and ER stress [13]. However, whether other molecules of the UPR

Electronic supplementary material The online version of this article (doi:10.1007/s12011-016-0668-5) contains supplementary material, which is available to authorized users.

✉ Xiao-Qiang Cong
congxiaoqiang@hotmail.com

[1] Department of Cardiology, Bethune First Hospital of Jilin University, 71 Xinmin St., Chaoyang District, ChangChun 130021, China

[2] Department of Anesthesiology, Bethune First Hospital of Jilin University, 71 Xinmin St., Chaoyang District, Changchun, Jilin 130021, China

[3] The People's Hospital of Jilin Province, Changchun 130021, China

[4] School of Public Health, Jilin University, Changchun 130021, China

pathway are also involved in diabetic cardiac cell apoptosis has not been reported.

The beneficial effects of vanadium have been widely studied in diabetic conditions mainly due to its insulin-mimicking effects of hypoglycemia [14–18]. Vanadium compounds exhibit long-lasting effects of anti-diabetic effects independent of the insulin receptor [19–21]. As vanadium salts are poorly ingested, organo-vanadium complexes were synthesized to increase uptake in the intestinal lining. Bis(maltolato) oxovanadium (IV) (BMOV) is one of such species to achieve anti-diabetic effects at one half of the dosage of vanadium salts, with minimal toxicity, and was shown to reverse the biochemical and morphological changes in diabetic models [18, 22–26]. Particularly, vanadate was shown to improve cardiac performance in diabetic animals [22] and can inhibit the ERS-induced increase in GRP78 and CHOP expressions at both messenger RNA (mRNA) and protein levels [27]. Given the antioxidant effects of BMOV [28, 29] and the essential roles of ROS and ERS in diabetic cardiac cell death [6, 7, 12, 28, 30–32], we assumed that BMOV antagonizes apoptosis in the diabetic heart by suppressing ERS and the subsequent activation of UPR. In this study, we have evaluated this assumption in both high glucose-treated cardiac cells and the hearts of diabetic rat models.

Materials and Methods

Ethics Statement

All animal procedures were reviewed and approved by Institutional Animal Care and Use Committee of the Institute of Zoology, Chinese Academy of Sciences (permit number IOZ11012) and by the Ethics Committee of Jilin University University. All researchers and students had received appropriate training and certification before performing animal studies. The use of research animals comply with the research to the Principles of Laboratory Animal Care (NIH publication #85-23, revised in 1985).

Cell Cultures and Treatments

The rat cardiomyoblast cell line H9C2 cells (American Type Culture Collection, Manassas, VA, USA) were maintained in Dulbecco's modified Eagle's medium (DMEM) supplemented with 10 % fetal bovine serum (FBS). The cultures were exposed to high glucose (30 mmol/l, Sigma) or 5.5 mmol/l D-glucose as control. To exclude a hyperosmolar effect, an equal concentration of mannitol (Sigma) was added to the control culture. At 2 h after high glucose treatment, BMOV (10 μM) was added. In experiments for terminal deoxynucleotidyl transferase-mediated dUTP nick-end labeling (TUNEL) assay, 4′,6-diamidino-2-phenylindole (DAPI) staining, and annexin-fluorescein isothiocyanate (FITC) apoptosis assay, the cells were grown in chamber slides. After high glucose exposure for 24 h, the monolayer cultures were collected after phosphate-buffered saline (PBS) washing and trypsinization treatment.

Diabetic Rat Model

Type II diabetic rats were induced as described with modifications [33]. Male SD rats weighed (250–280 g) were randomly divided into two groups: normal control group (6) and high-fat diet group (HFD, 12). All animals were fed with diet and water ad libitum. The normal control group was fed with regular diet; high-fat group was fed with a high-fat diet containing 20 % fat and 20 % sucrose. Animals were raised at ambient temperature of 22~27 °C, with 12/12 h day/night cycle. After 4 weeks of feeding, both group of animals were fasted (with water) for 16 h. Afterwards, the HFD group rats received a single intraperitoneal injection of low-dose STZ (45 mg/kg) in 0.1 mol/l bacteria-free citrate buffer, pH 4.4. The normal control group received a single injection of equal volume of 0.1 mol/l sterile citrate buffer. At 72 h after STZ injection, 6 ml blood was drawn from each animal (fasted 16 h of food but not water) and kept in coagulant tubes, centrifuged at low temperature (4 °C, 3500 r/min) for 7 min, and the serum was separated and kept at −20 °C. Fasting blood glucose (FBG) levels were measured. Animals with FBG levels higher than 10.0 mM/l and insulin sensitivity index (ISI = 22.5 / [FBG × INS], HOMA method) less than that of normal rats were determined as diabetic rats. During the experiment, all diabetic rats were continued to be fed with high-fat diet, while the normal control rats were fed with normal diet.

The experimental group rats were divided into BMOV group (6) and non-BMOV group. For the BMOV group, the rats received 6.22 mg BMOV/l in drinking water, reaching a daily supply of 10 μmol/kg day. In all cases, the BMOV solution was prepared daily. Weight gain and blood glucose were monitored weekly. For measurement of blood glucose, blood sample was taken from the tail vein, collected in sterilized tubes, and kept at 4 °C. After separation of serum by centrifuging, blood glucose was measured by the glucose oxidase method. Four weeks after the injection of STZ or vehicle, the animals were euthanized, and the heart were collected and rapidly frozen in liquid nitrogen for Western blot assays. For TUNEL staining, animals were perfused with 4 % paraformadehyde in PBS, followed by paraffin-embedding in 6-μm section. All animal procedures were approved by the Animal Care Committees of the University.

Western Blots

Cultured cells were rinsed twice with ice-cold PBS and lysed on ice in 10 volume lysis buffer (65 mM Tris·HCl, pH 6.8, 2 % sodium dodecyl sulfate (SDS), 2 % 2-mercaptoethanol, and 5 % glycerol, 30 min) containing 1 mM phenylmethylsulfonyl fluoride (PMSF) and centrifuged for 15 min, 12,000 rpm at 4 °C. Supernatants were stored at −80 °C for further experiments. Frozen tissue samples (hearts) were ground on dry ice and added 200 μl lysis buffer containing PMSF for every 10 mg tissue, sonicated, and lysed for 30 min on ice. The samples were centrifuged for 15 min, 12,000 rpm at 4 °C. The supernatants were stored at −80 °C for further use.

Protein concentration of the samples was measured by Coomassie Brilliant Blue G250 and was adjusted to the same level (6~8 μg/μl). An equal 50 μg protein samples in 5× loading buffer (containing β-mercaptoethanol) were loaded and run in electrophoresis on a 5 and 15 % separating SDS-polyacrylamide gel and then transblotted onto PVDF membranes (Merck Millipore) with a standard wet transferring apparatus (Bio-Rad). The membranes were blocked in Tris-buffered saline with Tween 20 (TBST) buffer (0.1 % Tween 20 and 5 % skim milk) at room temperature for 60 min. After three washes in TBST (15 min each), the membranes were incubated at 4 °C overnight in TBST containing primary antibodies diluted as per instructions (usually 1:1000). After three washes (15 min each) in TBST, blots were incubated with HRP-labeled sheep anti-mouse or sheep anti-rabbit IgG (1:5000; BOSTER, Pleasanton, CA, USA) in TBST buffer for 1 h. Antigens were detected by the BeyoECL Plus enhanced chemiluminescence system (Beyotime Institute Biotech, Jiangsu, China).

Apoptosis-TUNEL Assay

Apoptosis was detected on the paraffin sections using the Roche in situ cell death TUNEL assay kit of Converter-POD. Paraffin sections were dewaxed in water and dehydrated. Enzyme antigen was retrieved using proteinase K 10–20 μg/ml in 10 mM Tris–HCl (pH 7.4–7.8), 37 °C incubation for 20 min. The slides were washed in PBS twice (5 min each). Added TUNEL reaction mixture (enzyme solution/label solution = 1:9) on the slides, covered with film, incubated at 37 °C for 60 min. Added Converter-POD solution, incubated at 37 °C for 30 min. Sections were developed using DAB substrate with H_2O_2 in PBS. Counterstaining of DAPI was performed for some slides. The slides were washed for three times (5 min) with PBS after each step. Apoptotic cell deaths was visualized and counted under light microscope (Olympus BX51). Cells with stained nuclei were determined by counting 100 cells in three randomly selected fields.

Flow Cytometric Detection of Apoptosis

Early apoptosis in H9C2 cells were identified by double fluorescence staining using the Annexin V-FITC/PI Apoptosis Kit according to the instructions (Invitrogen). The cells were harvested after digestion with EDTA-free trypsin and centrifugation, washed twice with pre-cooled PBS, and centrifuged again at 300×*g*, 4 °C for 5 min, and 1~5 × 10^5 cells were collected. The cells were resuspended in 100 μl 1× binding buffer and added 5 μl annexin V-FITC and 5 μl PI staining solution and mixed gently, and the mixture reacted for 10 min in the dark at room temperature. Four hundred microliters of 1× binding buffer was added and mixed gently. Within 1 h, cellular fluorescence was measured by flow cytometry analysis with a FACSCalibur flow cytometer (BD Biosciences, USA).

Statistical Analysis

All data are expressed as means ± SD from at least three independent experiments. The differences were analyzed by ANOVA, followed by post hoc analysis with Student–Newman–Keuls test. Statistical significance was considered at $P < 0.05$.

Results

BMOV Inhibits Elevated Expression of the UPR Pathway Proteins in Cultured Cardiac H9C2 Cells

We examined the protein expression of the UPR signaling pathways in cultured H9C2 cells. High glucose treatment for 24 h dramatically enhanced the expression of almost all the UPR pathway-related proteins, except ATF6, TRAF2, and caspase 12 (Fig. 1). Addition of BMOV to the culture solution at 2 h after high glucose treatment significantly suppressed the enhanced expression of almost all the examined proteins, with some being completely restored, such as EIf2a, GRP78, caspase 3, ATF4, and CHOP. These results indicate that upon high glucose stimulation, the UPR pathways were fully activated and can be mostly suppressed by BMOV treatment.

BMOV Antagonize Apoptosis in Cultured H9C2 Cells Induced by High Glucose

High glucose treatment was shown to cause apoptosis in cultured H9C2 cells and in cardiac tissue of diabetic animal models. Consistently, we detected a high rate of apoptosis in both H9C2 cells (29.4 ± 1.2 %, Fig. 2), which was significantly reduced by the treatment of BMOV (22.8 ± 1.3 %, $P < 0.01$; Fig. 2a–b). The apoptosis assay of annexin-FITC similarly detected increased apoptosis in the high glucose-treated H9C2 cells, which was also attenuated by BMOV (Fig. 3).

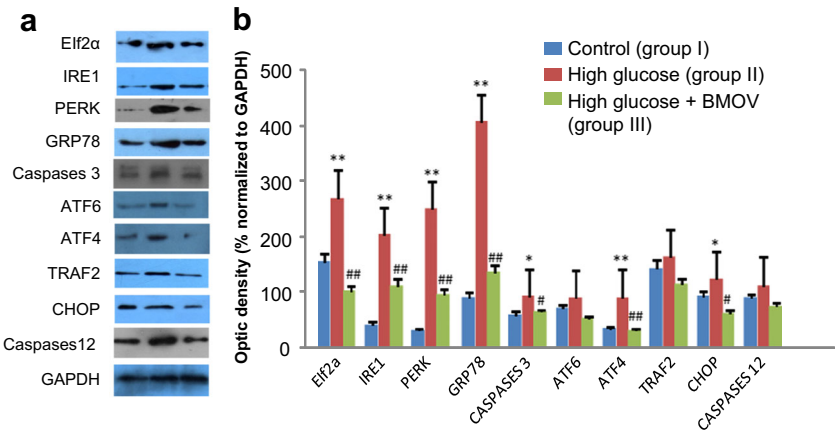

Fig. 1 Effects of high glucose and BMOV on UPR pathway protein expression in cultured H9C2 cells. **a** Representative Western blot of various URS-related proteins. **b** Normalized optic density (average and SE) of UPR pathway protein expression corresponding to **a**. All values were normalized to the density of GAPDH (% of GAPDH). The averages were summarized from five experimental repeats for each group. Group I is the control group; group II is the high glucose-treated cells; group III is the high glucose-treated cells plus BMOV. $^{*}P<0.05$, $^{**}P<0.01$ compared with group I. $^{\#}P<0.05$, $^{\#\#}P<0.01$ comparing between groups II and III

BMOV Counteracts Blood Sugar Level and Body Weight Increment in STZ Diabetic Rats

We monitored body weight and blood glucose levels weekly in STZ diabetic rats, control rats, and diabetic rats treated with BMOV. As shown in Fig. 4, both blood glucose levels (Fig. 4a) and body weight (Fig. 4b) were greatly increased in STZ-induced diabetic rats. The blood sugar increase started soon after STZ injection and reached a plateau level at week 2, while body weight gradually increased during the 4-week observation. Treatment of BMOV significantly ameliorated, but not completely reversed, the increment of both blood sugar level and body weight.

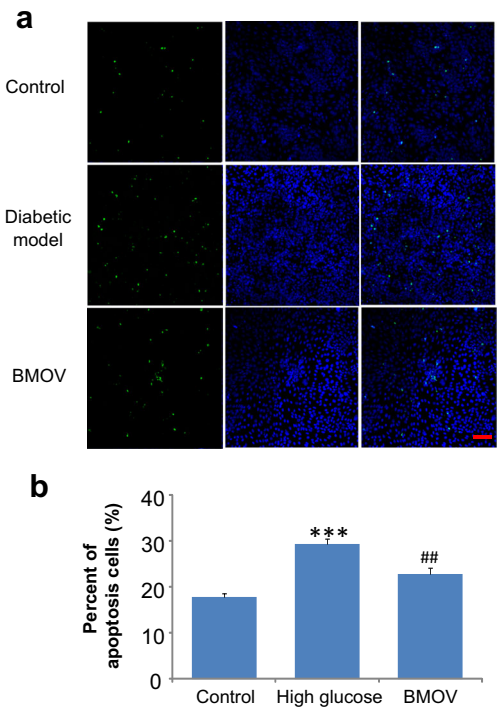

Fig. 2 TUNEL staining showing the high glucose-induced apoptosis in cultured H9C2 cells, which was attenuated by the treatment of BMOV. **a** Representative images of TUNEL staining showing the effects of high sugar and BMOV on apoptosis. *Green*, TUNEL stain; DAPI counterstain. **b** Summary of the effects of high sugar and BMOV on relative apoptosis rate (*bars*). $^{***}P<0.001$ compared with control cells; $^{\#\#}P<0.01$ compared with high glucose-treated cells

BMOV Suppressed Expression of the UPR Pathway Proteins in the Hearts of Diabetic Rats

We then examined the protein expression of the UPR signaling in the cardiac tissue of diabetic rat model by Western blot. Like in the H9C2 cells, most of the UPR pathway proteins showed increased expression in the STZ diabetic rats and were mostly completely inhibited by the treatment of BMOV (Fig. 5). The expression profiles were highly similar to those in H9C2 cells. Noticeably, in both the H9C2 cells and the hearts of diabetic rats, the expression of ATF6 and TRAF2 was not significantly altered. However, there was some slight difference in the expression patterns of UPR pathway proteins between the H9C2 cells and the hearts of diabetic rats, in that the expression of IRE1 and PERK was not significantly changed in the diabetic animals.

BMOV Alleviated Apoptosis in the Hearts of Diabetic Rats

Apoptotic cell deaths have been observed in the cardiac tissues of STZ-induced diabetic animal models [1, 3–5]. Consistently, using TUNEL assay, we detected a high ratio of apoptotic cells in the cardiac tissue of the STZ diabetic rats (20.5 ± 2.3 %, Fig. 6b, d). As in the H9C2 cells, treatment of BMOV effectively counteracted apoptosis in the hearts of the diabetic rats (5.4 ± 0.4 %, $P<0.001$; Fig. 6c–d).

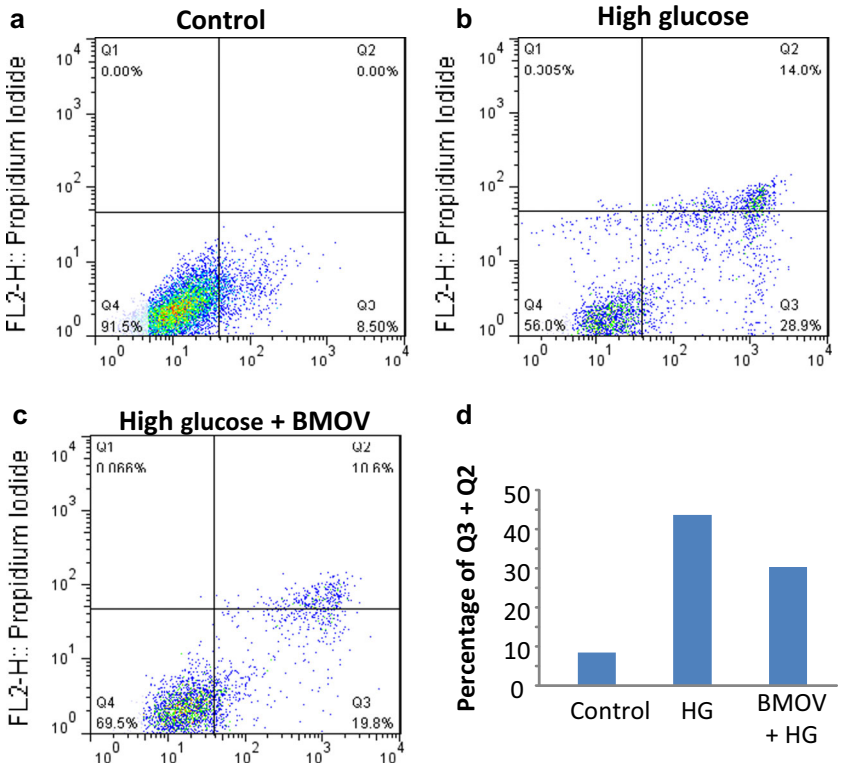

Fig. 3 Annexin V-FITC/PI double staining assay showing BMOV suppressed high glucose (HG)-induced apoptosis in cultured H9C2 cardiac cells. The degree of apoptotic cell death was quantified. Q4, Q3, and Q2 represent live cells, early apoptotic cells, and late apoptotic/necrosis cells, respectively. Data represent mean ± SD of three independent experiments

Discussion

In the current study, we show that in both high glucose-treated H9C2 cells and the hearts of the STZ rats, most of the UPR signaling molecules were significantly upregulated, together with a high rate of apoptotic cell deaths. Treatment of BMOV not only suppressed the overall enhanced expression of UPR pathway proteins but also significantly attenuated the apoptosis in both diabetic systems. These results provide further evidence for the crucial roles of ERS-activated UPR signaling in diabetic cardiomyopathy and suggest that BMOV alleviates apoptotic cardiac cell deaths in diabetes via suppression of activated UPR signaling.

The glucose-regulated protein, GRP78, was significantly increased in both the high glucose-treated cardiac cells and in the hearts of STZ rats, being particularly high in the cultured cells. GRP78 normally binds to the three initiators (PERK, IRE1, and ATF6) of UPR signaling to inhibit the UPR (Fig. 7), but is dissociated from these molecules upon ERS and results in the activation of UPR. The GRP78 protein regulates ER homeostasis by a variety of mechanisms: protein folding and assembly, targeting misfolded protein for degradation and ER Ca^{2+} binding, etc. It is considered a protector against ER stress, and the elevated expression in the two diabetic conditions is presumably a negative feedback protection mechanism. The particularly high expression in the H9C2 cells is possibly due to the direct effect of glucose, as it is a glucose-regulated protein.

The UPR signaling can be of either pro-survival or apoptotic. It is believed that the UPR initially restores normal ER functions by halting protein translation and increasing the generation of molecular chaperones to promote protein folding. However, prolonged disruption of ER functions by ER stress or when the restoration of ER functions could not be restored within a certain time lapse, the apoptotic pathway would be turned on [6, 34, 35]. To be survival or apoptotic also depends on the different UPR pathways. As illustrated in Fig. 7, there are three branches of the UPR signaling, initiated by PERK, ATF6, and IRE1α, respectively. The signaling cascade of PERK/EIf2α/ATF4/CHOP is of solely apoptotic, while the ATF6-initiated signaling is mainly pro-survival, and the IRE1α signaling may be either pro-survival or apoptotic which is further branched in three directions: the apoptotic pathways of TRAF/JNK and caspases 12/9/3 and the survival signaling of XBP1.

Our results show that in both diabetic systems, expression of ATF6 and TRAF2 was not increased, suggesting that the survival signaling of ATF6 and the apoptotic signaling of TRAF/JNK may not be activated. In high glucose-treated cardiac cells, both PERK and IRE1α were greatly increased, along with elevation of the corresponding downstream signaling molecules: EIf2α, ATF4, CHOP, and caspase 3. Among those, the elevation of PERK/EIf2/ATF4/CHOP signaling was more apparent comparing to that of caspases (no significant increase of caspase 12), suggesting that the PERK/EIf2/ATF4/CHOP signaling cascade is the major apoptotic UPR signaling in the H9C2 cells.

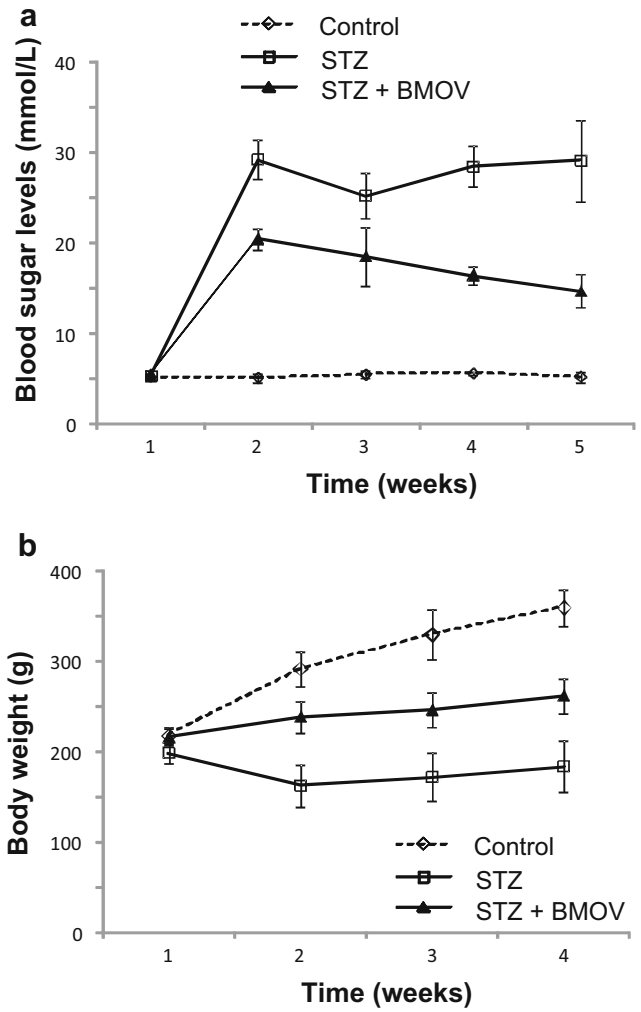

Fig. 4 Significantly increased blood sugar levels of hyperglycemia (**a**) and reduced body weight (**b**) in streptozotocin (STZ) diabetic rats. Administration of BMOV significantly and partially alleviated the hyperglycemia and the reduction of body weight (**b**) in STZ rats. Each data point represents mean ± SD of five animals

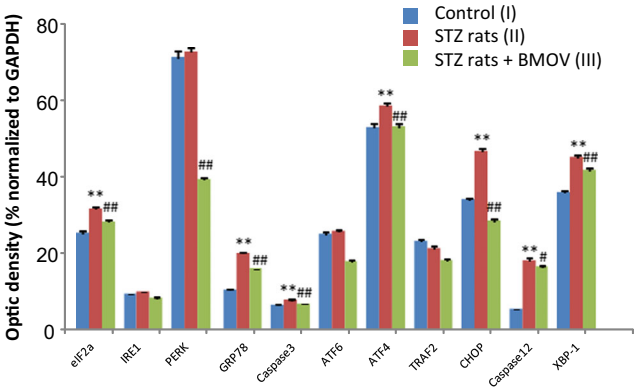

Fig. 5 Elevated expression of UPR signaling pathway proteins in the hearts of STZ diabetic rats that was suppressed by BMOV. The *data bars* represent the optic density (average density ± SE) of Western blot staining of the UPR pathway proteins normalized to that of GAPDH. The averages were summarization of five animals for each group. $^{*}P<0.05$, $^{**}P<0.01$ comparing between control and STZ rats; $^{\#}P<0.05$, $^{\#\#}P<0.01$ comparing between STZ rats and the STZ rats + BMOV groups

In the hearts of STZ rats, a significant change of PERK expression was not observed, while the expressions of EIf2α, ATF4, and CHOP were significantly elevated, indicating that the EIf2α/ATF4/CHOP signaling is also pivotal for the pathogenesis of cardiac cell deaths in the animal model. Comparing to the H9C2 cells, however, a remarkable increase in the expression of caspase 12 was detected besides the significant increase of caspase 3. Thus, it appears that in the STZ rats, the caspases also play an important role in diabetic cardiomyopathy. Presumably, with prolonged disruption of ER functions in the STZ rats, more apoptotic signaling is involved.

Regardless of the dominating apoptotic signaling and considerable apoptosis, the survival signals appear to be remained. In high glucose-treated H9C2 cells, we observed an increase of the spliced XBP1 mRNA (supplementary data, Fig. S1). In the hearts of STZ rats, the XBP1 protein expression was also elevated. In addition, the GRP78 protein was significantly upregulated in both diabetic conditions. Thus, despite the significant amount of apoptosis, the cardiac cells did not give up restoring the normal ER functions even under prolonged disruption of ER functions.

Vanadate may directly suppress the UPR signaling or indirectly via counteracting ROS and ER stress. For example, BOMV have been shown to be a strong antioxidant and exerted inhibiting effects on ERS [27, 36, 37]. Gao et al. [38] reported that vanadyl bisacetylacetonate (2.5 μM) protected pancreatic β cells from palmitate-induced cell death by further enhancement of GRP78 and downregulation of CHOP and subsequent insulin mRNA degradation. Their findings suggest that vanadate, at the concentration of 10 μM or less, may act directly on the UPR signaling to protect the pancreatic β cells. In another study, however, vanadate inhibited the ERS-induced increase in GRP78 and CHOP expressions at both mRNA and protein levels in glial cells [27]. These results suggest that in different cells, BMOV may exert different effects on the UPR signaling.

Our data show that BMOV counteracted the overall activation of UPR pathways in high glucose-treated H9C2 cells and in the hearts of STZ rats, including both the apoptotic and survival (GRP78 and XBP1) signaling. Therefore, the suppression may be the results of inhibition of the upstream of UPR signaling, possibly via inhibition of ROS and ERS, given the strong antioxidant activity of BMOV [36, 37]. As the apoptotic pathways were the dominating signaling in these conditions, the final consequence of BMOV administration was the attenuation of cardiac cell deaths.

Besides suppression of ROS and ER stress, vanadium compounds exhibited multiple insulin-mimicking effects, such as hypoglycemia (lowering plasma glucose levels, increasing

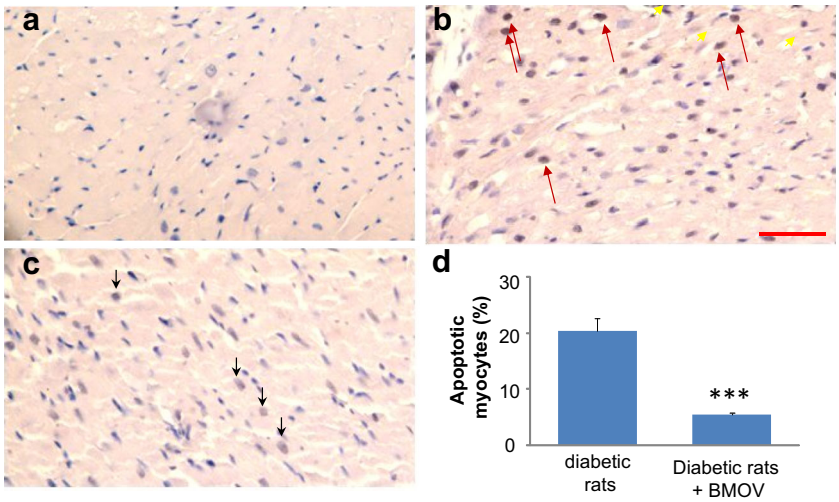

Fig. 6 TUNEL staining showing that BMOV attenuated apoptosis in the hearts of diabetic rats. **a** Control animals and **b** diabetic animals; *red arrows* show the TUNEL-positive cells; **c** diabetic animals treated with BMOV. Shown by the *arrows* are the TUNEL-positive cells that are more lightly stained compared to those in diabetic rats in **b. d** Summary of the effects of high sugar and BMOV on relative apoptosis rate (five animals for each group). Note that no apoptotic cell death was observed in the control animals and therefore no summarized data for this group. ***$P < 0.001$ compared with diabetic animals. Bar (*red* in B) = 100 μm

peripheral glucose uptake, and improving insulin sensitivity), decreased plasma lipid levels, and normalized liver enzyme activities [39]. These effects are likely to be mediated by the inhibition of tyrosine phosphatases and the subsequent activation of non-receptor protein tyrosine kinase (PTK) [40]. These actions, however, may not be related to the suppression of UPR protein expression of BMOV in the H9C2 cells, where there is no issues of lipids, liver enzymes, or

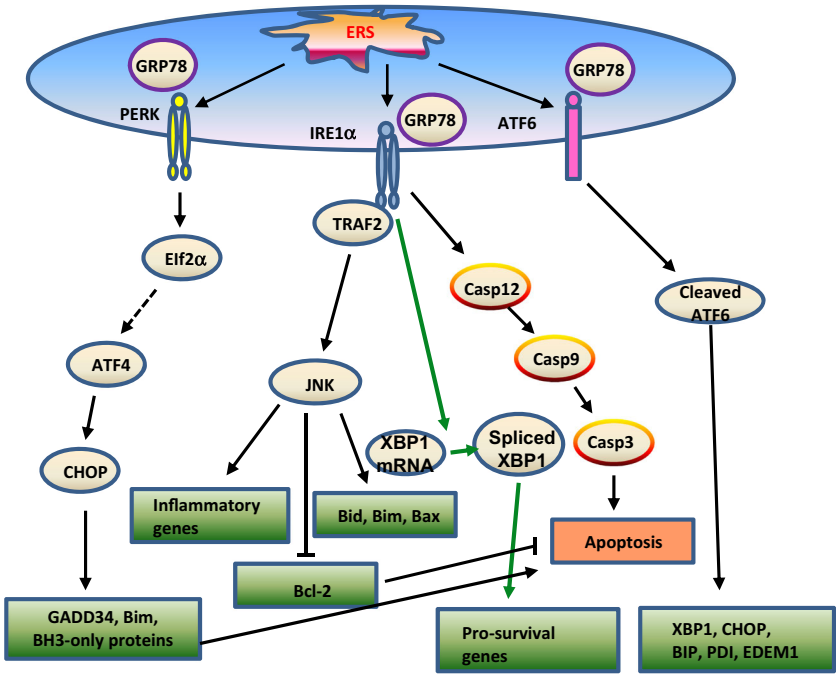

Fig. 7 A diagram showing the ERS-activated UPR signaling pathways. The ERS-induced accumulation of unfolded proteins results in the dissociation of GRP78 from the three target molecules at the ER membrane: PERK, IRE1a, and ATF6, triggering the activation of the three branches of UPR signaling. The different branches of the UPR signaling have different roles. GRP78 and XBP1 are the major survival signals. The PERK/EIf2α/ATF4/CHOP is solely of apoptotic, while the ATF6 is mainly of pro-survival, and the IRE1α can be both apoptotic (TRAF2/JNK and caspases 12/9/3) and pro-survival (XBP1). *GRP78* glucose-regulated protein 78, *ATF* activating transcription factor, *CHOP* C/EBP-homologous protein, *eIF-2α* eukaryotic translation initiation factor 2α, *ER* endoplasmic reticulum, *IRE1* inositol-requiring protein 1, *JNK* c-Jun N-terminal kinase, *PERK* pancreatic eIF-2α, *TRAF2* tumor necrosis factor receptor-associated factor 2, *XBP1* X-box binding protein 1, *Casp* caspase

plasma glucose level. Moreover, there is no evidence that the activation of PTK is related to the suppression of ROS and UPR signaling. However, it was shown that hyperglycemia and high plasma lipid can lead to ER stress and UPR [41, 42]. Therefore, it is possible that in the STZ animals, the suppression of ROS and UPR activation by BMOV could be an indirect effect of hypoglycemia and reduction of plasma lipid levels.

Taken together, we demonstrated that in both the high glucose-treated cardiac cells and in the hearts of STZ diabetic rats, there was an overall activation of the UPR signaling, which is predominantly apoptotic. However, pro-survival signaling still exists despite considerable amount of apoptosis, arguing against a single mode of apoptotic UPR signaling upon prolonged disruption of ER functions.

The administration of BMOV suppressed both the apoptotic and pro-survival UPR signaling, and the overall effect was the attenuation of the apoptotic cell deaths, suggesting that BMOV protects diabetic cardiomyopathy by counteracting ROS and ER stress. Our findings lend support to promote the use of BMOV in the treatment of diabetic heart diseases.

Acknowledgments The study is supported by The Health and Family Planning Commission of Jilin Province grant No. 2012Z095 to Cong XQ.

Compliance with Ethical Standards

Conflict of Interest None declared

References

1. Cai L, Kang YJ (2003) Cell death and diabetic cardiomyopathy. Cardiovasc Toxicol 3:219–228
2. Janka HU (1996) Increased cardiovascular morbidity and mortality in diabetes mellitus: identification of the high risk patient. Diabetes Res Clin Pract 30(Suppl):85–88
3. Adeghate E (2004) Molecular and cellular basis of the aetiology and management of diabetic cardiomyopathy: a short review. Mol Cell Biochem 261:187–191
4. Cai L, Li W, Wang G, Guo L, Jiang Y, Kang YJ (2002) Hyperglycemia-induced apoptosis in mouse myocardium: mitochondrial cytochrome C-mediated caspase-3 activation pathway. Diabetes 51:1938–1948
5. Pappachan JM, Varughese GI, Sriraman R, Arunagirinathan G (2013) Diabetic cardiomyopathy: pathophysiology, diagnostic evaluation and management. World J Diabetes 4:177–189. doi:10.4239/wjd.v4.i5.177
6. Xu J, Zhou Q, Xu W, Cai L (2012) Endoplasmic reticulum stress and diabetic cardiomyopathy. Exp Diabetes Res 2012:827971. doi:10.1155/2012/827971
7. Yang L, Zhao D, Ren J, Yang J (2014) Endoplasmic reticulum stress and protein quality control in diabetic cardiomyopathy. Biochim Biophys Acta. doi:10.1016/j.bbadis.2014.05.006
8. Li Z, Zhang T, Dai H, Liu G, Wang H, Sun Y, Zhang Y, Ge Z (2007) Involvement of endoplasmic reticulum stress in myocardial apoptosis of streptozocin-induced diabetic rats. J Clin Biochem Nutr 41:58–67. doi:10.3164/jcbn.2007008
9. Lakshmanan AP, Harima M, Suzuki K, Soetikno V, Nagata M, Nakamura T, Takahashi T, Sone H, Kawachi H, Watanabe K (2013) The hyperglycemia stimulated myocardial endoplasmic reticulum (ER) stress contributes to diabetic cardiomyopathy in the transgenic non-obese type 2 diabetic rats: a differential role of unfolded protein response (UPR) signaling proteins. Int J Biochem Cell Biol 45:438–447. doi:10.1016/j.biocel.2012.09.017
10. Liu ZW, Zhu HT, Chen KL, Dong X, Wei J, Qiu C, Xue JH (2013) Protein kinase RNA-like endoplasmic reticulum kinase (PERK) signaling pathway plays a major role in reactive oxygen species (ROS)-mediated endoplasmic reticulum stress-induced apoptosis in diabetic cardiomyopathy. Cardiovasc Diabetol 12:158. doi:10.1186/1475-2840-12-158
11. Ozturk N, Olgar Y, Ozdemir S (2013) Trace elements in diabetic cardiomyopathy: an electrophysiological overview. World J Diabetes 4:92–100. doi:10.4239/wjd.v4.i4.92
12. Varga ZV, Giricz Z, Liaudet L, Hasko G, Ferdinandy P, Pacher P (2014) Interplay of oxidative, nitrosative/nitrative stress, inflammation, cell death and autophagy in diabetic cardiomyopathy. Biochim Biophys Acta. doi:10.1016/j.bbadis.2014.06.030
13. Younce CW, Wang K, Kolattukudy PE (2010) Hyperglycaemia-induced cardiomyocyte death is mediated via MCP-1 production and induction of a novel zinc-finger protein MCPIP. Cardiovasc Res 87:665–674. doi:10.1093/cvr/cvq102
14. Badmaev V, Prakash S, Majeed M (1999) Vanadium: a review of its potential role in the fight against diabetes. J Altern Complement Med 5:273–291
15. Heyliger CE, Tahiliani AG, McNeill JH (1985) Effect of vanadate on elevated blood glucose and depressed cardiac performance of diabetic rats. Science 227:1474–1477
16. Kopp SJ, Daar J, Paulson DJ, Romano FD, Laddaga R (1997) Effects of oral vanadyl treatment on diabetes-induced alterations in the heart GLUT-4 transporter. J Mol Cell Cardiol 29:2355–2362. doi:10.1006/jmcc.1997.0469
17. Nandhini D, Maneemegalai S, Elangovan V, Sekar N, Govindasamy S (1993) Insulin-like effects of bis-glycinato oxovanadium (IV) complex on experimental diabetic rats. Indian J Biochem Biophys 30:73–76
18. Noda C, Masuda T, Sato K, Ikeda K, Shimohama T, Matsuyama N, Izumi T (2003) Vanadate improves cardiac function and myocardial energy metabolism in diabetic rat hearts. Jpn Heart J 44:745–757
19. Fantus IG, Ahmad F, Deragon G (1994) Vanadate augments insulin-stimulated insulin receptor kinase activity and prolongs insulin action in rat adipocytes. Evidence for transduction of amplitude of signaling into duration of response. Diabetes 43:375–383
20. Mooney RA, Bordwell KL, Luhowskyj S, Casnellie JE (1989) The insulin-like effect of vanadate on lipolysis in rat adipocytes is not accompanied by an insulin-like effect on tyrosine phosphorylation. Endocrinology 124:422–429. doi:10.1210/endo-124-1-422
21. Ui M, Okada T, Hazeki K, Hazeki O (1995) Wortmannin as a unique probe for an intracellular signalling protein, phosphoinositide 3-kinase. Trends Biochem Sci 20:303–307
22. Clark TA, Deniset JF, Heyliger CE, Pierce GN (2014) Alternative therapies for diabetes and its cardiac complications: role of vanadium. Heart Fail Rev 19:123–132. doi:10.1007/s10741-013-9380-0
23. Clark TA, Maddaford TG, Tappia PS, Heyliger CE, Ganguly PK, Pierce GN (2010) Restoration of cardiomyocyte function in streptozotocin-induced diabetic rats after treatment with vanadate in a tea decoction. Curr Pharm Biotechnol 11:906–910
24. Winter CL, Lange JS, Davis MG, Gerwe GS, Downs TR, Peters KG, Kasibhatla B (2005) A nonspecific phosphotyrosine phosphatase inhibitor, bis(maltolato)oxovanadium(IV), improves glucose tolerance and prevents diabetes in Zucker diabetic fatty rats. Exp Biol Med (Maywood) 230:207–216

25. Yuen VG, Orvig C, Thompson KH, McNeill JH (1993) Improvement in cardiac dysfunction in streptozotocin-induced diabetic rats following chronic oral administration of bis(maltolato)oxovanadium(IV). Can J Physiol Pharmacol 71: 270–276
26. Yuen VG, Vera E, Battell ML, Li WM, McNeill JH (1999) Acute and chronic oral administration of bis(maltolato)oxovanadium(IV) in Zucker diabetic fatty (ZDF) rats. Diabetes Res Clin Pract 43:9–19
27. Hosoi T, Saito A, Kume A, Okuma Y, Nomura Y, Ozawa K (2008) Vanadate inhibits endoplasmic reticulum stress responses. Eur J Pharmacol 594:44–48. doi:10.1016/j.ejphar.2008.07.034
28. Rahimi R, Nikfar S, Larijani B, Abdollahi M (2005) A review on the role of antioxidants in the management of diabetes and its complications. Biomed Pharmacother 59:365–373. doi:10.1016/j.biopha.2005.07.002
29. Saxena AK, Srivastava P, Kale RK, Baquer NZ (1993) Impaired antioxidant status in diabetic rat liver. Effect of vanadate. Biochem Pharmacol 45:539–542
30. Cai L, Kang YJ (2001) Oxidative stress and diabetic cardiomyopathy: a brief review. Cardiovasc Toxicol 1:181–193
31. Ozcan U, Yilmaz E, Ozcan L, Furuhashi M, Vaillancourt E, Smith RO, Gorgun CZ, Hotamisligil GS (2006) Chemical chaperones reduce ER stress and restore glucose homeostasis in a mouse model of type 2 diabetes. Science 313:1137–1140. doi:10.1126/science.1128294
32. Xu J, Wang G, Wang Y, Liu Q, Xu W, Tan Y, Cai L (2009) Diabetes- and angiotensin II-induced cardiac endoplasmic reticulum stress and cell death: metallothionein protection. J Cell Mol Med 13:1499–1512. doi:10.1111/j.1582-4934.2009.00833.x
33. Reed MJ, Meszaros K, Entes LJ, Claypool MD, Pinkett JG, Gadbois TM, Reaven GM (2000) A new rat model of type 2 diabetes: the fat-fed, streptozotocin-treated rat. Metabolism 49:1390–1394. doi:10.1053/meta.2000.17721
34. Iwakoshi NN, Lee AH, Vallabhajosyula P, Otipoby KL, Rajewsky K, Glimcher LH (2003) Plasma cell differentiation and the unfolded protein response intersect at the transcription factor XBP-1. Nat Immunol 4:321–329. doi:10.1038/ni907ni907
35. Ma Y, Hendershot LM (2001) The unfolding tale of the unfolded protein response. Cell 107:827–830
36. Krejsa CM, Nadler SG, Esselstyn JM, Kavanagh TJ, Ledbetter JA, Schieven GL (1997) Role of oxidative stress in the action of vanadium phosphotyrosine phosphatase inhibitors. Redox independent activation of NF-kappaB. J Biol Chem 272:11541–11549
37. Shah DI, Singh M (2006) Inhibition of protein tyrosin phosphatase improves vascular endothelial dysfunction. Vasc Pharmacol 44: 177–182. doi:10.1016/j.vph.2005.11.004
38. Gao Z, Zhang C, Yu S, Yang X, Wang K (2011) Vanadyl bisacetylacetonate protects β cells from palmitate-induced cell death through the unfolded protein response pathway. J Biol Inorg Chem 16:789–798. doi:10.1007/s00775-011-0780-0
39. Shechter Y, Shisheva A (1993) Vanadium salts and the future treatment of diabetes. Endeavour 17:27–31
40. Shisheva A, Shechter Y (1992) Quercetin selectively inhibits insulin receptor function in vitro and the bioresponses of insulin and insulinomimetic agents in rat adipocytes. Biochemistry 31:8059–8063
41. Bravo R, Parra V, Gatica D, Rodriguez AE, Torrealba N, Paredes F, Wang ZV, Zorzano A, Hill JA, Jaimovich E, Quest AFG, Lavandero S (2013) Endoplasmic reticulum and the unfolded protein response: dynamics and metabolic integration. Int Rev Cell Mol Biol 301:215–290. doi:10.1016/b978-0-12-407704-1.00005-1
42. Lu Y, Cheng J, Chen L, Li C, Chen G, Gui L, Shen B, Zhang Q (2015) Endoplasmic reticulum stress involved in high-fat diet and palmitic acid-induced vascular damages and fenofibrate intervention. Biochem Biophys Res Commun 458:1–7. doi:10.1016/j.bbrc.2014.12.123